J Membrane Biol (2011) 240:13–20
DOI 10.1007/s00232-011-9338-x

# Calcium Inhibits Dihydropyridine-Stimulated Increases in Opening and Unitary Conductance of a Plant $Ca^{2+}$ Channel

**Miguel A. Piñeros · Mark Tester**

Received: 26 March 2010 / Accepted: 2 January 2011 / Published online: 28 January 2011


We have previously characterized the "RCA" channel (root $Ca^{2+}$ channel), a voltage-dependent, $Ca^{2+}$-permeable channel found in plasma membrane-enriched vesicles from wheat roots incorporated into artificial planar lipid bilayers. Earlier work indicated that this channel was insensitive to 1,4-dihydropyridines (DHPs, such as nifedipine and 202–791). However, the present study shows that this channel is sensitive to DHPs, but only with submillimolar $Ca^{2+}$, when the probability of channel opening is reduced, with flickery closures becoming increasingly evident as $Ca^{2+}$ activity decreases. Under these ionic conditions, addition of nanomolar concentrations of (+) 202–791 or nifedipine caused an increase in both the probability of channel opening and the unitary conductance. It is proposed that there is a competitive interaction between $Ca^{2+}$ and DHPs at one of the $Ca^{2+}$-binding sites involved in $Ca^{2+}$ permeation and that binding of a DHP to one of the $Ca^{2+}$-permeation sites facilitates movement of other calcium ions through the channel. The present study shows that higher plant $Ca^{2+}$-permeable channels can be greatly affected by very low concentrations of DHPs and that channel sensitivity may vary with the ionic conditions of the experiment. The results also indicate interesting structural and functional differences between plant and animal $Ca^{2+}$-permeable channels.

M. A. Piñeros (✉)
Robert W. Holley Center for Agriculture and Health, United States Department of Agriculture-Agricultural Research Service, Cornell University, Ithaca, NY 14853-2901, USA
e-mail: map25@cornell.edu

M. Tester
Australian Centre for Plant Functional Genomics and University of Adelaide, Private Mail Bag 1, Glen Osmond, Adelaide, SA 5064, Australia

**Keywords** Dihydropyridine · Calcium · Unitary conductance · Single-channel recording

## Introduction

Depolarization- and hyperpolarization-activated $Ca^{2+}$ channels mediate $Ca^{2+}$ influx into plant cells. The physiological role, the selectivity and the pharmacological profiles of plant $Ca^{2+}$ channels often differ significantly from their animal counterparts. Most notably, these plant channels are permeable to, rather than selective for, $Ca^{2+}$ (for comprehensive reviews, see Demidchik et al. 2002; Hetherington and Brownlee 2004). We have reported the main biophysical (e.g., conductivity, selectivity and permeability) and pharmacological characterization of the "RCA" (root $Ca^{2+}$) channel, a voltage-dependent, $Ca^{2+}$-permeable channel recorded from wheat root plasma membrane-enriched fractions (Piñeros and Tester 1995, 1997a, b; White et al. 2000). The voltage dependence of the RCA indicates that this channel is closed by hyperpolarizing voltages, while remaining open at depolarizing voltages. The biochemical and electrophysiological evidence strongly supports the plasma-membrane origin for this channel. The type of pore structure, the permeation and selectivity mechanisms and the pharmacological properties described for this channel indicate strong structural and functional similarities between this higher plant $Ca^{2+}$ channel and $Ca^{2+}$ channels in the membranes of animal cells, namely, L-type. However, other functional properties—such as the RCA channel having a significant permeability to cations which are relatively impermeant ($Mg^{2+}$, $Mn^{2+}$) or which block L-type $Ca^{2+}$ channels in animal cells ($Cd^{2+}$, $Co^{2+}$, $Ni^{2+}$) and/or the lower affinity for the binding of $Ca^{2+}$ to the two $Ca^{2+}$ intrapore-binding sites (White et al. 2000)—also indicate significant

differences between the RCA structure compared with those in calcium channels in animal cells.

Given the thorough understanding of the structure and function of $Ca^{2+}$ channels in animal cells gained through extensive use of organic compounds that modulate the activity of these channels (Hockerman et al. 1997), such compounds have also been used with plant $Ca^{2+}$ channels in an attempt to elucidate any structural and functional similarities which may be shared between $Ca^{2+}$-permeable channels from both types of organism. A general lack of specificity to certain of these pharmacological agents, as demonstrated, e.g., by the blocking of $K^+$ plant channels by some of the so-called $Ca^{2+}$ channel blockers (see, e.g., Terry et al. 1992; Thomine et al. 1994), has called into question the existence of specific high-affinity binding sites in plant $Ca^{2+}$-permeable channels. The direct effects of the compounds on the putative plasma membrane and tonoplast plant $Ca^{2+}$-permeable channels have rarely been corroborated at the single-channel level and, even then, only with use of relatively high concentrations of the compounds (10–100 μM). Among the two groups of compounds used most frequently (the phenylalkylamines and the 1,4-dihydropyridines, DHPs), functional evidence has already been obtained for the existence of an intrapore phenylalkylamine receptor in at least one higher plant $Ca^{2+}$-permeable channel ($K_{½}$ at 0 mV of 24 μM (Piñeros and Tester 1997b)). By contrast, the functional pharmacological evidence for DHP receptors remains contradictory. For example, while tracer flux and electrophysiological studies (e.g., Marshall et al. 1994; Klüsener et al. 1995; Huang et al. 1994) have suggested that higher plant $Ca^{2+}$-permeable channels lack DHP receptors, other studies have shown both antagonistic and agonistic effects by DHPs (e.g., Allen and Sanders 1994; Very and Davies 2000; Gelli and Blumwald 1997).

Although previous results indicated that the RCA channel lacks DHP receptors (Piñeros and Tester 1997a), the present work shows that this channel is in fact sensitive to DHPs but only under particular ionic conditions (notably, low $Ca^{2+}$). The results suggest that DHPs, as well as $Ca^{2+}$, regulate the kinetics and permeation of the channel by interacting with intrapore binding sites involved in the permeation of $Ca^{2+}$ through this plant $Ca^{2+}$-permeable channel. The details of these interactions have been found to be quite different in plant and animal channels.

## Materials and Methods

### Membrane Isolation, Planar Lipid Bilayers and Channel Reconstitution

RCA channel reconstitution from enriched plasma-membrane vesicles from wheat roots and single-channel data acquisition were performed as described in Piñeros and Tester (1995, 1997a, b). Pharmacological results presented in the later publications indicated the extracellular face of the RCA channel is exposed to the *cis* chamber. The conductivity, selectivity and permeability characteristics of the RCA channel in ionic environments simulating physiological conditions (i.e., low and high cytoplasmic $Ca^{2+}$ and $K^+$ activities, respectively) have been established previously (Piñeros and Tester 1997a). In the present study, all recordings were conducted in simple $CaCl_2$ unbuffered solutions, with the pH adjusted to 5.5 by addition of HCl. All organic channel effectors were dissolved in ethanol at concentrations that ensured that no more than 4% ethanol was present in the extracellular solution; this concentration of ethanol had no effect on channel activity. The concentrations of ethanol and DHPs had no effect on the pH of the solution.

### Single-Channel Recordings and Data Analysis

Single-channel currents were recorded under voltage-clamp conditions using a Dagan 3900A amplifier (with a 3910 expander; Dagan, Minneapolis, MN), connected to the bilayer chambers via 3 M KCl/1% agar salt bridges. Analog signals were filtered at 100 Hz with an eight-pole low-pass Bessel filter (series 902; Frequency Devices, Haverhill, MA) and digitized at 2 kHz using PCLAMP 6.0 software (Axon Instruments, Foster City, CA). Voltages were measured in the outside chamber (*trans* side) with respect to the cup (*cis* side), following the convention used for intact cells (i.e., cytosol with respect to the outside). Membrane potentials were stepped from zero to the desired voltage. Movement of $Ca^{2+}$ from the *cis* to the *trans* chamber is indicated by a negative current and is shown as a downward deflection in the current traces (as for an inward current in intact cells). Steady-state open-state probabilities ($P_o$) were calculated as a ratio of total open time to the total recording time and derived from amplitude histograms as described by Bertl and Slayman (1990). Recordings of 3–5 min duration were used for analyses. In cases where two channels were present in the same bilayer, the following probability formula was used: $P_o = (A_1 + 2A_2)/2(A_0 + A_1 + A_2)$, where $A_1$ and $A_2$ represent the total open time for one and two channels, respectively, $A_0$ represents the total time with both channels closed and $P_o$ represents the open probability of a single channel. Single-channel traces and current–frequency distributions indicated the presence of a subconductance state (e.g., see distribution in Fig. 2b). Given the small number of representative events of this subconductance state (relative to those of the closed and full opening states), it was not feasible to accumulate a large number of events to generate representative dwell-time histograms of this state. Thus,

although additional open or closed states might be present, given the above limitations, the reaction scheme used to describe the kinetics of the RCA channel consisted of only one open and one closed state, with the channel considered to be in its open state during the subconductance state. Mean time constants were estimated only from recording (as those shown in Fig. 2), where only one channel was inserted in the bilayer. Recordings showing any indication of two or multiple channels were discarded. Mean time constants were estimated from dwell-time logarithmic histogram distributions with square-root ordinates of the open and closed states as described by Sigworth and Sine (1987), using the Simplex and Levenberg–Marquardt least squares method provided by PCLAMP 9.0 software. All other curve fittings were performed using Origin 7.5 software (OriginLab, Northampton, MA). Standard error bars represent the SEM and are shown only when larger than the symbol. As liquid junction potentials were very small (no more than ±2 mV), they were not taken into account. Each set of observations and ionic conditions was performed in at least two different bilayers. Ionic activities were estimated using the GEOCHEM-EZ speciation program (Shaff et al. 2010). DHPs were provided by Dr. P. Hof (Sandoz, Basel, Switzerland).

## Results

In our previous experiments on the wheat root voltage-dependent $Ca^{2+}$ (RCA) channel, biophysical properties such as $P_o$ were measured with extracellular $Ca^{2+}$ concentrations as low as 1 mM. Under these conditions, the channel showed a sharp voltage dependence (gating charge, $z$, of about 4.2), remaining open for long periods of time at holding potentials positive of −115 mV. As the holding potentials became more negative, the channel closed within seconds and remained in its closed state (Piñeros and Tester 1995). We were also able to resolve single-channel conductances at concentrations below 1 mM $Ca^{2+}$ (White et al. 2000). As shown in Fig. 1a, decreasing $Ca^{2+}$ resulted in a reduction in the single-channel current amplitude (i.e., unitary conductance) as well as a modification of the single-channel kinetics. Three different gating modes, resembling those described for single $Ca^{2+}$ channels from animal cells (Hess et al. 1984), could be resolved. "Mode 0" refers to the condition where the channel remains in the closed state. At low $Ca^{2+}$ (<100 μM), the open-state kinetics of the RCA channel resemble "mode 1," characterized by brief and "flickery" channel openings occurring in bursts. With higher $Ca^{2+}$ concentrations (e.g., 1 mM), the kinetics of the RCA channels shift to "mode 2," characterized by long-lasting channel openings and a high $P_o$. It is important to note that

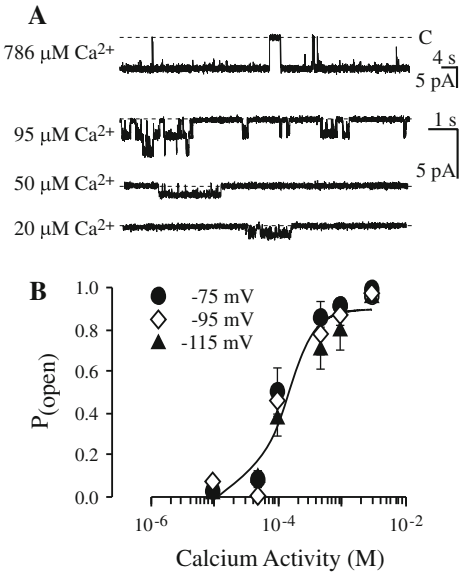


**Fig. 1** Effects of extracellular $Ca^{2+}$ concentration on $Ca^{2+}$ permeation and gating kinetics of RCA single-channel activity. **a** Currents through single channels clamped at −115 mV and exposed to symmetrical $CaCl_2$ activities indicated on the left margin. *Dashed lines* represent the current level when all channels were closed. Sample traces were taken from different bilayers and selected to illustrate changes in current amplitude and short-term gating kinetics. Note different time and current scales between the first trace and the bottom three traces. **b** Open probability ($P_{open}$) as a function of the symmetrical $Ca^{2+}$ activity present in the *cis* and *trans* sides of the channel. The open probabilities at the different holding potentials indicated by the *symbols* were estimated from recordings of 3–5 min duration as described in "Materials and Methods" section. The *smooth curve* was drawn for the −75-mV values according to the Hill equation $P_{open} = \{P_{o(max)} * [Ca^n/(Ca^n + K^n)]\}$, where $P_{o(max)}$ is the maximum open probability, K is the $Ca^{2+}$ activity where $P_{open}$ reaches half its maximal value and Ca is the $Ca^{2+}$ activity. Best fit was obtained with $P_{o(max)} = 0.9$, $K = 120 \pm 20$ μM $Ca^{2+}$ and $n = 1.9 \pm 0.6$ ($R^2 = 0.972$)

the flickery closures apparent in the traces are not "shunt" noise arising from the very low $Ca^{2+}$ concentrations around the channel pore because they can be eliminated by addition of low concentrations of DHPs, as described later in this study. Thus, the flickering is a true effect of $Ca^{2+}$ on gating and not an effect on permeation arising from the low concentrations of $Ca^{2+}$ used in these experiments. Reducing $Ca^{2+}$ reduced the maximum $P_o$ at a given voltage (Fig. 1b). Analysis of $P_o$ as a function of $Ca^{2+}$ suggests that, in addition to permeating the channel, $Ca^{2+}$ was involved in an allosteric regulation of the channel, enhancing a conformational change to a more "active state" (e.g., mode 2). These results suggest a $Ca^{2+}$ binding site with a dissociation constant of 120 μM $Ca^{2+}$ (Fig. 1b). This value is of the same order of magnitude as the affinity of the channel for $Ca^{2+}$ permeation (i.e., 100 μM) reported previously (White et al. 2000; Piñeros and Tester 1997a, b).

In previous studies, the effect of DHPs was tested under ionic conditions where the RCA channel remained mainly

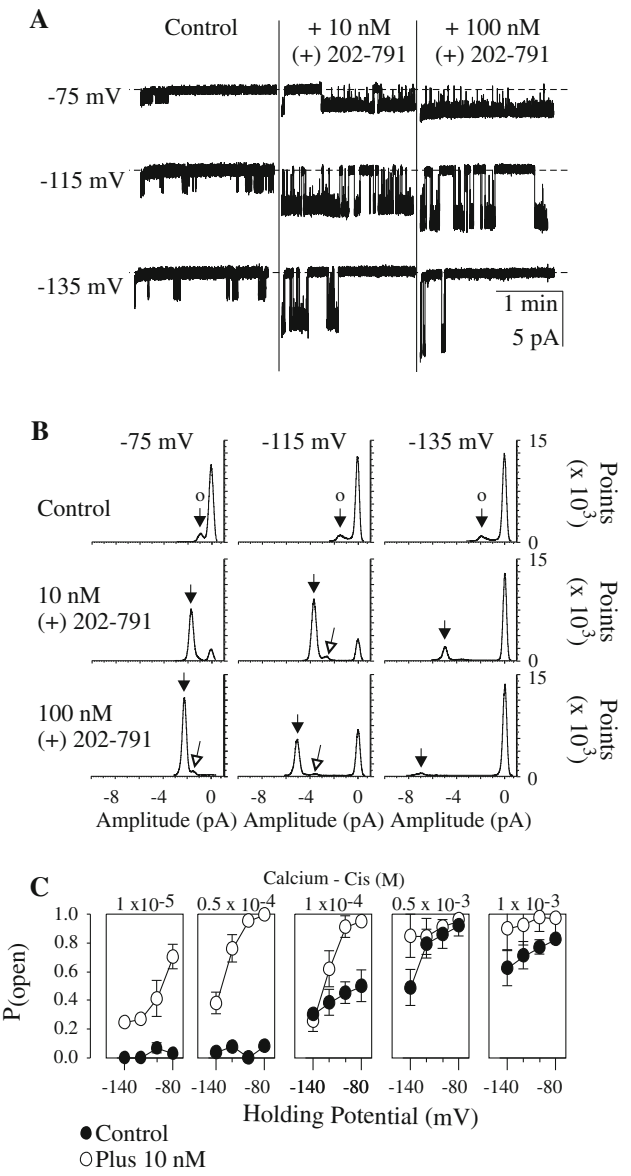


**Fig. 2** Changes in single-channel current amplitude and in channel kinetics in symmetrical $CaCl_2$ conditions upon exposure to the DHP (+) 202–791. **a** Example of single-channel recordings illustrating typical changes in single-channel kinetics and current amplitude upon exposure of the extracellular side (*cis*) to 10 and 100 nM DHP. Recordings were obtained in symmetrical 50 μM $CaCl_2$ at the voltages indicated on the *left margin* of each trace. *Dashed lines* represent the current level when the channel was closed. All traces from the same bilayer. **b** Effects of the DHP (+) 202–791 on the probability of channel opening. Examples of single-channel current–frequency distributions generated from long time recordings (sampling frequency of 2 kHz, bin size of 0.04 pA), as those shown in **a**. Recordings were obtained in symmetrical 50 μM $CaCl_2$ at the voltages indicated on the top of the panels under the conditions (absence and presence of 10 and 100 nM [+]202-791) denoted on the left-hand margin. *Closed arrow* at the top of each distribution indicates the open state of the channel. *Open arrow* (where present) illustrates the subconductance state described in the text. **c** Effects of 10 nM DHP (+) 202–791 on probability of channel opening at varying symmetrical $Ca^{2+}$ activities (as detailed at the *top* of each panel) and holding potentials (*bottom axis*). Open probabilities were estimated as described in "Materials and Methods" section

in mode 2 (i.e., high $P_o$ in >1 mM $Ca^{2+}$), concluding that DHPs had no effect on either single-channel kinetics or current amplitude (Piñeros and Tester 1997a). However, in the present study, we took advantage of the reduction in $P_o$ by low $Ca^{2+}$ to determine the sensitivity of the RCA channel to DHPs. Exposure of the extracellular side of the channel (in symmetrical 50 μM $Ca^{2+}$) to concentrations as low as 10 nM (+) 202–791 resulted in an increase in $P_o$ as mode 2 was clearly favored (Fig. 2a, b). A 10-fold increase in (+) 202–791 did not greatly increase $P_o$ (at 50 μM $Ca^{2+}$), suggesting the DHP-binding site was saturated at a lower concentration. More importantly, the addition of (+) 202–791 also increased the single-channel current amplitude. Analyses were performed only on inward currents as treatments on outward currents had no apparent effect. The effects of DHPs on the RCA single-channel currents were reversible upon perfusion of the *cis* chamber with control solutions. Prior to further analysis, it is worth noting that under all ionic conditions tested (including the absence of DHP) a subconductance state was regularly detected, being particularly evident at larger negative voltages. The current amplitude of this subconductance state was about 75% of that recorded during full channel opening (see single-channel current–frequency distribution in Fig. 2b).

Considering first the $Ca^{2+}$ dependence of the DHP-induced changes in $P_o$, exposure to 10 nM (+) 202–791 led to an increase in $P_o$ provided that the $Ca^{2+}$ concentrations surrounding the channel were low (Fig. 2c). At 500 μM and higher $Ca^{2+}$ concentrations, (+) 202–791 did not cause an increase in $P_o$. At lower $Ca^{2+}$ concentrations (10–100 μM), addition of 10 nM (+) 202–791 caused an increase in $P_o$. Lowering $Ca^{2+}$ concentrations resulted in a shift of the intrinsic voltage dependence of the channel to more negative potentials, such that the increases in $P_o$ following the addition of 10 nM (+) 202–791 were more accentuated at depolarized membrane potentials, where the RCA channel has a higher $P_o$ (as determined by the voltage sensor of the channel [Piñeros and Tester 1995]). It is worth noting that the apparent lack of voltage dependence at $Ca^{2+}$ concentrations of 500 μM and higher (in the absence of DHP) shown in Fig. 2c is due to the predominance of the open state at this range of holding potentials, under these specific ionic conditions.

The kinetics of the open, $\tau_{(Open)}$, and closed, $\tau_{(Closed)}$, times were also analyzed to further elucidate the mechanism by which $Ca^{2+}$ and (+) 202–791 modulated $P_o$. The presence of extracellular (+) 202–791 (at a given $Ca^{2+}$ concentration) led to a significant increase in $\tau_{(Open)}$ (Fig. 3a). In contrast, $\tau_{(Closed)}$ tended to remain unaffected (Fig. 3a). However, the lack of change in $\tau_{(Closed)}$ should be

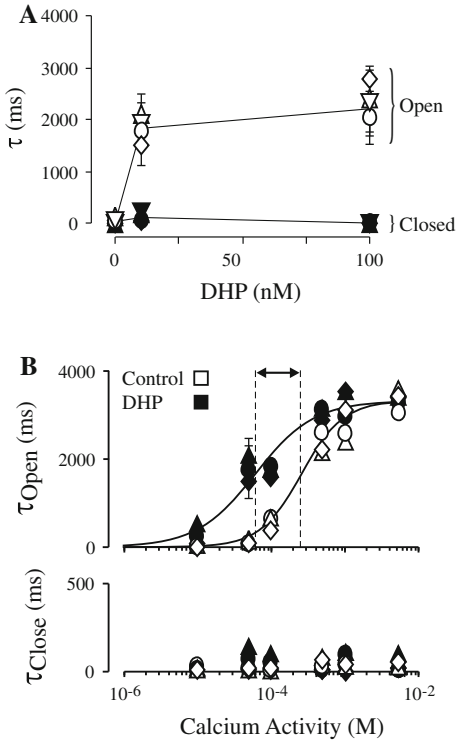


**Fig. 3** Dependence of the time constants of the open and closed states on the extracellular (*cis*) DHP (+) 202–791 and symmetrical $Ca^{2+}$ activities. **a** Dependence of time constants of the open (*open symbols*) and closed (*closed symbols*) states on extracellular (*cis*) 10 nM (+) 202–791. Values for four different membrane potentials (*rhomboids* = −75 mV, *circles* = −95 mV, *upward triangles* = −115 mV, *downward triangles* = −135 mV) are shown. Individual points represent the average from four different bilayers in symmetrical ionic conditions of 50 μM $CaCl_2$. Lines were drawn for clarity. **b** Dependence of the time constants of the open (*top panel*) and closed (*bottom panel*) states on the symmetrical extra and intracellular $Ca^{2+}$ activities (*x*-axis) in the absence (*open symbols*) and presence (*closed symbols*) of 10 nM (+) 202–791. *Values* are shown for four different membrane potentials (*symbols* correspond to those shown in **a**) representing the average from at least four different bilayers. *Smooth curves for the top panel* were drawn according to the Hill equation, $y = \tau_{(\text{Open max})} * [Ca^n/(Ca^n + K^n)]$, where $P_{o(max)}$ is the maximum open probability and K is the $[Ca^{2+}]$ where $\tau_{(\text{Open max})}$ reaches half its maximal value. Best fit for control values resulted in $\tau_{(\text{Open max})} =$ 3,300 ± 159 ms, K = 260 ± 40 μM $Ca^{2+}$ and $n = 1.54 + 0.23$ ($R^2 = 0.983$) and in $\tau_{(\text{Open max})} = 3{,}280 \pm 345$ ms, K = 60 ± 10 μM $Ca^{2+}$ and $n = 1.10 \pm 0.24$ for DHP values ($R^2 = 0.973$)

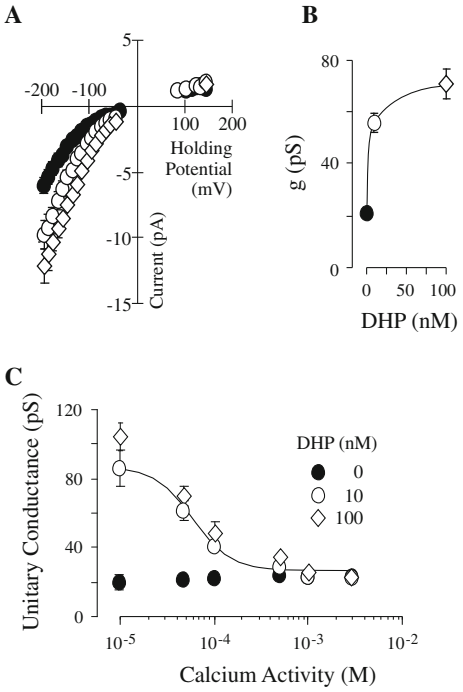


**Fig. 4** Unitary single-channel conductance increase upon exposure to (+) 202–791. **a** Unitary *I–V* relationships in the absence (*closed circles*) and presence of extracellular (*cis*) 10 (*open circles*) and 100 (*open diamonds*) nM (+) 202–791. Individual points represent the average of currents from at least four bilayers with symmetrical 50 μM $CaCl_2$. **b** Increase in single-channel unitary conductance with increasing concentrations of extracellular (*cis*) (+) 202–791. Symbols correspond to those shown for the *I–V* relationships in **a**. Unitary conductances were estimated from the slopes of the linear regressions of the data points between −145 and −45 mV of the data shown in **a**. *Smooth curve* was drawn for clarity. **c** Inhibition of the DHP-induced single-channel unitary conductance increase by increasing $Ca^{2+}$ activities. Curve drawn to the 10 nM (+) 202–791 data points corresponds to the sigmoidal curve $g = A_2 + (A_1 - A_2)/(1 + (X/X_0)^p)$, where *g* is the unitary conductance (pS), $A_1$ and $A_2$ are the initial and final values, respectively, and $X_0$ is the point of inflection. Best fit was obtained with 60 ± 5 μM $Ca^{2+}$, $A_1 = 87.6 \pm 2.9$ pS, $A_2 = 25.7 \pm 1.2$ pS and $p = 2.08 \pm 0.4$ ($R^2 = 0.995$)

treated cautiously as these values aggregate close to the filter cut-off (i.e., 100 Hz). The change in $\tau_{(\text{Open})}$ times is consistent with the significant (+) 202–791-induced increase in $P_o$ observed earlier at low $Ca^{2+}$ concentrations. Figure 3b describes the dependence of $\tau_{(\text{Open})}$ and $\tau_{(\text{Closed})}$ on $Ca^{2+}$ (i.e., the permeant ion) in the absence and presence of (+) 202–791. In the absence of (+) 202–791, increasing $Ca^{2+}$ led to an increase in $\tau_{(\text{Open})}$, with a $K_{1/2}$ of 260 ± 40 μM $Ca^{2+}$ reaching a value in $\tau_{(\text{Open max})}$ of about 3,300 ms. In the presence of (+) 202–791, increasing $Ca^{2+}$ also led to an increase in $\tau_{(\text{Open})}$, with $\tau_{(\text{Open max})}$ reaching similar values as in the absence of (+) 202–791 (i.e., 3,280). However, most notably, the $K_{1/2}$ value shifted to 60 ± 10 μM $Ca^{2+}$. The shift in the $Ca^{2+}$ $K_{1/2}$ dose–response curves upon addition (+) 202–791 is a clear indication of allosteric modulation between $Ca^{2+}$ and (+) 202–791.

The increase in single-channel conductance induced by extracellular (+) 202–791 is described in Fig. 4. As shown earlier (Fig. 2), exposure to (+) 202–791 caused an increase in the single-channel current amplitude recorded at a given voltage. Interestingly, the increase in current was observed only in the inward (i.e., negative) current. The increase in unitary conductance of the inward current elicited by (+) 202–791 was dependent on both the (+) 202–791 and the $Ca^{2+}$ concentrations surrounding the

channel. A 10-fold increase in (+) 202–791 concentration led to a modest increase in the unitary conductance (at a given $Ca^{2+}$ concentration). The (+) 202–791-induced increase in unitary conductance was inhibited in a concentration-dependent manner by the permeating ion (i.e., $Ca^{2+}$), with the increase being reduced as $Ca^{2+}$ concentrations increased. The (+) 202–791-induced increase in single-channel conductance was halved at $Ca^{2+}$ concentration of about 60 μM. This value is of the same order of magnitude as the $Ca^{2+}$ dissociation constant determining the $P_o$ (120 μM, Fig. 1b), as well as the $K_{½}$ for $Ca^{2+}$ permeation (100 μM [Piñeros and Tester 1997a; White et al. 2000]). These results reinforce the allosteric interactions taking place between $Ca^{2+}$ and (+) 202–791.

Exposure of the extracellular side of the channel to as little as 6 nM nifedipine (in low $Ca^{2+}$) also induced long channel openings and an increase in single-channel conductance (Fig. 5). The increase in single-channel current amplitude increased as the extracellular nifedipine concentration increased, saturating close to 100 nM nifedipine with a $K_{½}$ between 25 and 32 nM (Fig. 5). Increasing $Ca^{2+}$ concentrations attenuated the nifedipine effects in a manner similar to that described for (+) 202–791 (data not shown). It is worth noticing that the apparent lack of increase in $P_o$ at −135 and −155 mV following the addition of up to 500 nM nifedipine is due to the significant shift in intrinsic voltage dependence of the RCA channel at low $Ca^{2+}$ concentrations (i.e., 20 μM $Ca^{2+}$), as exemplified in Fig. 2c. Overall, the effects of nifedipine on the RCA channel indicate a generalized effect of DHPs on the RCA channel at low $Ca^{2+}$ concentrations.

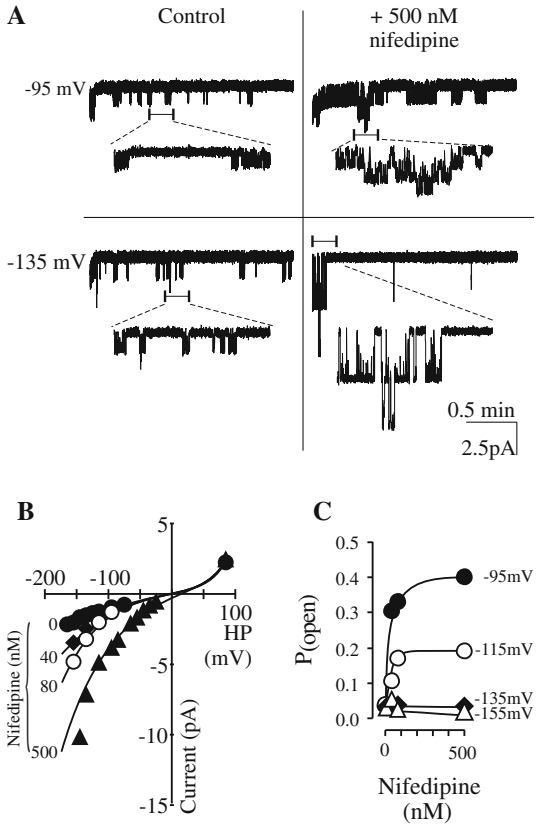


**Fig. 5** Effects of extracellular nifedipine on single RCA channel activity and current amplitude. **a** Example of single-channel recordings illustrating typical changes in single-channel current amplitude and kinetics upon exposure to 500 nM nifedipine. The example traces for two channels incorporated into one bilayer were recorded on the same bilayer at the voltages indicated on the left margin of each trace. Recordings were obtained in 20 μM $CaCl_2$ on the extracellular side (*cis*) and 50 μM $CaCl_2$ on the cytosolic (*trans*) side. For clarity, the trace sections indicated by the small *scale bars* have been enlarged and are presented *below* each trace. The time scale on the *bottom right* margin corresponds to the *upper* trace. **b** Unitary *I–V* relationship obtained in the absence (*filled circle*) and presence of 40 (*filled diamond*), 80 (*open circle*) and 500 (*filled diamond*) nM nifedipine. Individual points represent the average of currents measured from at least two observations. *Lines* were drawn for clarity. **c** Increase in probability of channel opening, $P_o$, with increasing concentrations of nifedipine at different voltages. The channel was exposed to 20 μM $CaCl_2$ on the extracellular side (*cis*) and 50 μM $CaCl_2$ on the cytosolic (*trans*) side. *Curves* were drawn according to the Hill equation, $P_o = P_{o(max)} * [Nif^n/(Nif^n + K^n)]$, where Nif stands for nifedipine, $P_{o(max)}$ is the maximum open probability and K is the Nif concentration where $P_o$ reaches half its maximal value. Best fits were obtained by setting $n = 1$, resulting in $P_{o(max)}$ 0.41 ± 0.04 and 0.18 ± 0.04 and $K_{½}$ 18 ± 10 and 17 ± 12 nM for the −95 mV ($R^2 = 0.829$) and −115 mV ($R^2 = 0.784$) sets of data, respectively

## Discussion

Compared with the extensive knowledge of the location and modes of action of DHP receptors in $Ca^{2+}$ channels in animal cells, any understanding of the structure of $Ca^{2+}$-permeable channels from plant cells remains only preliminary. Although the weight of evidence favors the absence of DHP receptors from higher plant plasma membranes, the present study shows that the effects of nanomolar concentrations of DHPs become evident when the wheat root voltage-dependent, $Ca^{2+}$-permeable channel (RCA) is exposed to extracellular micromolar $Ca^{2+}$ activities. Extracellular nanomolar concentrations of DHPs had two main effects on the RCA single-channel activity. First, DHPs stabilized the channel in its open state (or in gating modes that favor the open state), consequently increasing its $P_o$ at a given holding potential. Second, there was an increase in the single-channel unitary conductance. In order to reconcile this unique observation with previous work, it is necessary to understand the functional and structural properties of the RCA channel. For the RCA channel, White et al. (2000) proposed a pore structure in which $Ca^{2+}$ ions permeate in single file through a pore with three energy barriers and two intrapore binding sites with a high affinity for $Ca^{2+}$ (3B2S model). Although similar to other models proposed for several $Ca^{2+}$ channels in the

membranes of animal cells (Friel and Tsien 1989; Hess and Tsien 1984; Yellen 1993; Almers and McCleskey 1984), the affinity of $Ca^{2+}$ for the binding sites within the pore of the RCA channel is much lower than that in animal $Ca^{2+}$ channels. The model also indicates a considerable surface charge in the vestibules to the RCA channel pore, which can account partially for the high unitary conductances and rectification properties of the inward single-channel current recorded at low $Ca^{2+}$ concentrations.

The present study also indicated that, in addition to permeating the RCA channel, $Ca^{2+}$ plays a regulatory role in stabilizing the channel in its open state. The similarity between the dissociation constant of $Ca^{2+}$ for this stabilization (120 μM) and the $K_{½}$ for $Ca^{2+}$ permeation (100 μM) suggests two possible mechanisms for $Ca^{2+}$ regulation. The first is that at low $Ca^{2+}$ concentrations (below the $K_{½}$ for permeation), it would become increasingly likely that only one binding site would be occupied. Given that $Ca^{2+}$ permeation through the RCA pore requires the binding of two $Ca^{2+}$ ions, the probability of finding the channel in a nonconducting state would increase at low $Ca^{2+}$. This would appear as the "flickery" kinetics observed for the channel at low $Ca^{2+}$ concentrations. As the $Ca^{2+}$ concentration increases (above the $K_{½}$), the probability of $Ca^{2+}$ binding to two binding sites increases, thus stabilizing the channel in its conducting state and increasing its $P_o$. Alternatively, the binding of $Ca^{2+}$ to an allosteric site involved in channel gating (e.g., the voltage sensor) could stabilize the channel in its open state. Thus, the $Ca^{2+}$-binding sites could be distinct from, although clearly coupled to, the binding sites involved in permeation.

The DHP-induced changes in the RCA channel kinetics at low $Ca^{2+}$ concentrations can be reconciled using similar models to those described for $Ca^{2+}$ channels from animal cells. DHPs may act as channel agonists (stabilizing the open state) or antagonists (stabilizing the inactivated state). It is proposed that DHP antagonistic effects are due to a direct blocking of the permeation pathway within the channel pore as the DHP molecule appears to bind to two sites within the channel pore (Zhorov et al. 2001; Lipkind and Fozzard 2003; Peterson and Catterall 1995; Mitterdorfer et al. 1995). In the case of the RCA channel, addition of extracellular nanomolar concentrations of DHPs has an agonistic effect. While the RCA channel is found mainly in mode 0 (closed state) or 1 (short-lived openings) at low $Ca^{2+}$ concentrations, addition of DHPs favors the transition from either mode 0 or 1 to mode 2 (longer-lasting openings). Superimposed on the agonistic effects is an interaction of DHP with $Ca^{2+}$ as increasing $Ca^{2+}$ concentrations surrounding the RCA channel attenuated the DHP-induced changes in kinetics and current amplitude. Given the similarity in the $K_{½}$ for this $Ca^{2+}$ attenuation with that for $Ca^{2+}$ permeation and $Ca^{2+}$ stabilization of the stable open state (mode 2) of the RCA channel, it is likely that DHPs compete with $Ca^{2+}$ at either a regulatory or a permeation binding site. At low $Ca^{2+}$ concentrations, DHPs appear to mimic $Ca^{2+}$ binding to the $Ca^{2+}$-binding site, stabilizing the channel in its conducting state, resulting in agonistic activity. As the $Ca^{2+}$ concentration increases, the $Ca^{2+}$-binding site becomes occupied predominantly by $Ca^{2+}$, both stabilizing the open state and preventing DHP from binding. Similar DHP–$Ca^{2+}$ interactions have been reported in calcium channels from animal cells and described in a model whereby, depending on the number of $Ca^{2+}$ ions bound to the intrapore binding sites involved in $Ca^{2+}$ permeation, the DHP receptor can shift reversibly between three states with different affinities for binding DHPs (Hockerman et al. 1997; Mitterdorfer et al. 1995; Peterson and Catterall 1995, 2006).

Generally, agonists have been reported to have little or no effect on single-channel amplitude and selectivity (Coronado and Affolter 1986; Zhorov et al. 2001). To our knowledge, there are only two studies in cardiac $Ca^{2+}$ channels from animal cells that report an occasional slight increase in single-channel current amplitude due to the presence of DHPs (Kokubun and Reuter 1984; Lacerda and Brown 1989). In the present study we report the unique observation of a significant increase in single-channel current amplitude upon addition of extracellular DHPs. It should be noted that, under the filtering and sampling conditions used in the present study, the unitary conductance estimates could potentially be biased by the channel's fast gating in low-$Ca^{2+}$ conditions, particularly as the closure events become faster than the recording. However, the estimates for the unitary conductance of the RCA channel in the absence of DHP and in ionic conditions evoking fast gating were similar in magnitude to those estimated from recording in ionic conditions inducing slow gating (i.e., long-lasting channel openings in the absence of DHP and high $Ca^{2+}$). Furthermore, the fact that the addition of extracellular DHP led to a fivefold increase in unitary conductance, relative to that estimated from slow-gated recordings, substantiates the assertion that the changes in unitary conductance are the result of DHP–$Ca^{2+}$ interactions in the RCA channel. The DHP-induced increase in unitary conductance decreased as the $Ca^{2+}$ concentration increased, halving with $Ca^{2+}$ concentrations that were similar to both the $Ca^{2+}$–DHP interaction constant determined from the open probabilities and the $K_{½}$ for $Ca^{2+}$ permeation. The observed significant increase in conductivity supports the hypothesis that DHPs interact with at least one of the $Ca^{2+}$-binding sites involved in permeation, rather than with a "gating" regulatory site. It is proposed that at low $Ca^{2+}$ concentrations DHPs modify the permeation pathway within the RCA channel, allowing

$Ca^{2+}$ ions to permeate more rapidly through the pore, leading to an increase in unitary conductance. As the $Ca^{2+}$ concentrations increase, the permeation binding sites are preferentially occupied by $Ca^{2+}$, returning the permeation pathway to its original state. Thus, DHPs could modulate the channel kinetics and permeation by a mechanism that would alter the affinity of a permeation binding site(s). This would lead to changes in ion occupancy favoring double occupancy, thus stabilizing the channel in its permeable mode and allowing faster transport rates.

The present study has demonstrated that higher plant $Ca^{2+}$-permeable channels have at least one DHP receptor. Our results indicated that although some differences in DHP sensitivity, as measured in other studies, may be due to differences in membranes and species, studies involving channel sensitivity to DHPs should be treated cautiously as the channel sensitivity may vary with the ionic conditions of the experiment.

**Acknowledgements** We gratefully acknowledge financial support from an Australian Research Council Federation Fellowship (to M. T.)

## References

Allen GJ, Sanders D (1994) Two voltage-gated, calcium release channels coreside in the vacuolar membrane of broad bean guard cells. Plant Cell 6:685–694

Almers W, McCleskey EW (1984) Non-selective conductance in calcium channels of frog muscle: calcium selectivity in a single-file pore. J Physiol 353:585–608

Bertl A, Slayman CL (1990) Cation-selective channels in the vacuolar membrane of *Saccharomyces*: dependence on calcium, redox state, and voltage. Proc Natl Acad Sci USA 87:7824–7828

Coronado R, Affolter H (1986) Characterization of dihydropyridine-sensitive calcium channels from purified skeletal muscle transverse tubules. In: Miller C (ed) Ion channel reconstitution. Plenum Press, New York, pp 483–505

Demidchik V, Davenport RJ, Tester M (2002) Nonselective cation channels in plants. Annu Rev Plant Physiol Plant Mol Biol 53:67

Friel DD, Tsien RW (1989) Voltage-gated calcium channels: direct observation of the anomalous mole fraction effect at the single-channel level. Proc Natl Acad Sci USA 86:5207–5211

Gelli A, Blumwald E (1997) Hyperpolarization-activated $Ca^{2+}$-permeable channels in the plasma membrane of tomato cells. J Membr Biol 155:35–45

Hess P, Tsien RW (1984) Mechanism of ion permeation through calcium channels. Nature 309:453–456

Hess P, Lansman JB, Tsien RW (1984) Different modes of Ca channel gating behaviour favoured by dihydropyridines Ca agonists and antagonists. Nature 311:538–544

Hetherington A, Brownlee C (2004) The generation of $Ca^{2+}$ signals in plants. Annu Rev Plant Biol 55:401–427

Hockerman GH, Peterson BZ, Johnson AB, Catterall WA (1997) Molecular determinants of drug binding and action on L-type calcium channels. Annu Rev Pharmacol Toxicol 37:361–396

Huang JW, Grunes DL, Kochian LV (1994) Voltage-dependent $Ca^{2+}$ influx into right-side-out plasma membrane vesicles isolated from wheat roots: characterization of a putative $Ca^{2+}$ channel. Proc Natl Acad Sci USA 91:3473–3477

Klüsener B, Boheim G, Liá H, Engelberth J, Weiler EW (1995) Gadolinium-sensitive, voltage-dependent calcium release channels in the endoplasmic reticulum of a higher plant mechanoreceptor organ. EMBO J 14:2708–2714

Kokubun S, Reuter H (1984) Dihydropyridine derivatives prolong the open state of Ca channels in cultured cardiac cells. Proc Natl Acad Sci USA 81:4824–4827

Lacerda AE, Brown AM (1989) Nonmodal gating of cardiac calcium channels as revealed by dihydropyridines. J Gen Physiol 93: 1243–1273

Lipkind GM, Fozzard HA (2003) Molecular modeling of interactions of dihydropyridines and phenylalkylamines with the inner pore of the L-type $Ca^{2+}$ channel. Mol Pharmacol 63:499–511

Marshall J, Corzo A, Leigh RA, Sanders D (1994) Membrane potential-dependent calcium transport in right-side-out plasma membrane vesicles from *Zea mays* L. roots. Plant J 5:683–694

Mitterdorfer J, Sinnegger MJ, Grabner M, Striessnig J, Glossmann H (1995) Coordination of $Ca^{2+}$ by the pore region glutamates is essential for high-affinity dihydropyridine binding to the cardiac $Ca^{2+}$ channel a1 subunit. Biochemistry 34:9350–9355

Peterson BZ, Catterall WA (1995) Calcium binding in the pore of L-type calcium channels modulates high affinity dihydropyridine binding. J Biol Chem 270:18201–18204

Peterson BZ, Catterall WA (2006) Allosteric interactions required for high-affinity binding of dihydropyridine antagonists to CaV1.1 channels are modulated by calcium in the pore. Mol Pharmacol 70:667–675

Piñeros M, Tester M (1995) Characterization of a voltage-dependent $Ca^{+2}$-selective channel from wheat roots. Planta 195:478–488

Piñeros M, Tester M (1997a) Calcium channels in higher plant cells: selectivity, regulation and pharmacology. J Exp Bot 48:551–577

Piñeros M, Tester M (1997b) Characterization of the high-affinity verapamil binding site in a plant plasma membrane $Ca^{2+}$-selective channel. J Membr Biol 157:139–145

Shaff JE, Schultz BA, Craft EJ, Clark RT, Kochian LV (2010) GEOCHEM-EZ: a chemical speciation program with greater power and flexibility. Plant Soil 330:207–214

Sigworth FJ, Sine SM (1987) Data transformations for improved display and fitting of single-channel dwell time histograms. Biophys J 52:1047–1054

Terry BR, Findlay GP, Tyerman SD (1992) Direct effects of $Ca^{2+}$-channel blockers on plasma membrane cation channels *Amaranthus tricolor* protoplasts. J Exp Bot 43:1457–1473

Thomine S, Zimmermann S, Van Duijn B, Barbier-Brygoo H, Guern J (1994) Calcium channel antagonists induce direct inhibition of the outward rectifying potassium channel in tobacco protoplasts. FEBS Lett 340:45–50

Very AA, Davies JM (2000) Hyperpolarization-activated calcium channels at the tip of *Arabidopsis* root hairs. Proc Natl Acad Sci USA 97:9801–9806

White PJ, Piñeros M, Tester M, Ridout MS (2000) Cation permeability and selectivity of a root plasma membrane calcium channel. J Membr Biol 174:71–83

Yellen G (1993) Structure and selectivity. Nature 366:109–110

Zhorov BS, Folkman EV, Ananthanarayanan VS (2001) Homology model of dihydropyridine receptor: implications for L-type $Ca^{2+}$ channel modulation by agonists and antagonists. Arch Biochem Biophys 393:22–41